REPORT 520

AGARD

ADVISORY GROUP FOR AEROSPACE RESEARCH & DEVELOPMENT

64 RUE DE VARENNE PARIS 7E FRANCE

Correlation of wind-tunnel and flight-test aerodynamic data for five V/STOL aircraft

by D. H. Hickey and W. L. Cook

★

OCTOBER 1965

NORTH ATLANTIC TREATY ORGANIZATION

REPORT 520

NORTH ATLANTIC TREATY ORGANIZATION

ADVISORY GROUP FOR AEROSPACE RESEARCH AND DEVELOPMENT

CORRELATION OF WIND-TUNNEL AND FLIGHT-TEST AERODYNAMIC DATA FOR FIVE V/STOL AIRCRAFT

by

David H. Hickey and Woodrow L. Cook

This Report is one of the series 515-522 of papers presented at the 27th meeting of the AGARD Flight Mechanics Panel, held 11-12 October 1965 in Rome, Italy

SUMMARY

The five aircraft tested represent a wide variety of V/STOL concepts. Correlation between the wind-tunnel and flight-test aerodynamic results is generally good when wind-tunnel wall corrections are omitted; in some cases wall corrections are shown to degrade the correlation. The aircraft and wind-tunnel geometry are related to model-tunnel sizing parameters and a VTOL lift parameter, in order to establish tentative sizing criteria for V/STOL wind-tunnel testing with small wall effects.

SOMMAIRE

Les cinq avions essayés représentent une grande diversité de conceptions V/STOL. La corrélation entre les résultats aérodynamiques d'essais dans le tunnel et ceux en vol est bonne dans l'ensemble quand on omet les corrélations de parois du tunnel aérodynamique; on constate dans certains cas que les corrections de paroi dégradent la corrélation. On apparente la géométrie des appareils et du tunnel aérodynamique aux paramètres de calibrage de modèle-tunnel et à un paramètre de portance VTOL, afin d'établir des critères de calibrage provisoires pour les essais en tunnel aérodynamique V/STOL avec faibles effets de paroi.

533.6.071
:533.652.6

CONTENTS

LIST OF TABLES

LIST OF FIGURES

NOTATION

A_L area of VTOL lifting element, $n(\pi D_L^2/4)$, ft^2

A_m momentum area of aircraft, $\pi b^2/4$, ft^2

A_T wind-tunnel cross-section area, ft^2

b wing span, ft

b_T tunnel width, ft

D_L diameter of lifting element

h_T tunnel height, ft

L lift, lb

n number of propellers, fans, or rotors

T_F fan thrust, lb

V airspeed, knots

V_j jet velocity, knots

CORRELATION OF WIND-TUNNEL AND FLIGHT-TEST AERODYNAMIC DATA FOR FIVE V/STOL AIRCRAFT

David H. Hickey and Woodrow L. Cook*

1. INTRODUCTION

For the general improvement of V/STOL state-of-the-art and the development of useful V/STOL concepts and configurations, it is essential to have accurate wind-tunnel test data. Very little experimental information is available for defining the geometric relationship between model and wind tunnel and the momentum relationships between the propulsive forces and the wind-tunnel air flow necessary for keeping wall effects small in wind-tunnel test data for the transition speed range of V/STOL type aircraft.

The large angularities in the flow field around V/STOL aircraft make it difficult to correct wind-tunnel data for wall effects. The only available theoretical treatment for correcting potential flow of this type is that of Reference 1. This theory is complex, however, and because of its fundamental assumptions is difficult to apply to all V/STOL configurations. The assumption of a uniformly loaded lifting element across the span, as on a helicopter rotor, needs considerable modification before it can be applied to V/STOL aircraft that have highly concentrated lifting elements at various points across the span. The assumption that the wake of the lifting element goes directly to the tunnel floor without any deflection or bending due to forward velocity can have a significant bearing on the magnitude of calculated wall effects because the average wake deflection angle would be considerably greater; consequently the calculated wall effects would be less with a downstream wake defection included. The theory has been verified experimentally[2] for a low disk loading helicopter rotor, and also wall effects have been examined[3-5] by testing a model in various sized wind tunnels and correlating the results with theoretical wind-tunnel wall effects obtained by modifying the theory of Reference 1.

In this report the effects of wall constraints are examined by a different approach. Full-scale wind-tunnel aerodynamic test results are compared with flight results for aircraft representing several V/STOL concepts and tentative boundaries for model to wind-tunnel size parameters are indicated. The interrelationship of scale effect, experimental techniques, and wall effects is discussed.

2. DESCRIPTION OF TEST AIRCRAFT

Aircraft dimensions pertinent to the calculation of wind-tunnel wall corrections are presented in Table 1. Further details of the individual aircraft follow.

2.1 Bell XV-3

The XV-3 convertiplane, shown in Figure 1, is a conventional configuration which has 23 ft diameter helicopter rotors mounted on masts at each wing tip. While hovering,

---

*Ames Research Center, NASA, Moffett Field, California, USA

the aircraft functions as a helicopter with helicopter type controls. In order to attain wing-supported flight speed, the rotor masts are tilted forward until the rotor axis is alined with the flight path. Further details of the aircraft are given in Reference 6.

2.2 Ryan VZ-3

The VZ-3 (Fig. 2) used an extensive flap system to deflect propeller flow downward to attain VTOL capability. VTOL controls consisted of a combination of propeller pitch controls, slipstream controls, and reaction control from the residual thrust of the turboshaft engine. The transition from hover to conventional flight is accomplished by varying flap deflection (and propeller slipstream deflection provide thrust for acceleration. Further details of the aircraft are presented in Reference 7.

2.3 Chance Vought-Ryan-Hiller XC-142

The XC-142 (a 0.6 scale model is shown in Figure 3) is a tilt-wing aircraft with four engines and four propellers. The aircraft uses full-span flaps to help deflect the propeller slipstream and reduce the wing tilt required. Hover controls consist of variable-pitch propeller controls, slipstream controls, and a tail-mounted rotor for pitch control. Wing-supported flight speed is obtained by reducing wing tilt and flap deflection. Wing-tunnel data presented herein are from the 0.6 scale model[8]. Model power limitations caused the test airspeed to be reduced to about one-half of the full-scale value. This is the only aircraft in this program that was too large to be tested in the wind-tunnel.

2.4 Lockheed XV-4A

The XV-4A (Fig. 4) is powered by two jet engines which exhaust vertically through an ejector in the fuselage for VTOL lift and exhaust normally for cruise thrust. Hover, pitch, and yaw control is supplied by the reaction from tail pipe bleed, and roll control from compressor bleed. Blowing boundary-layer control is also used to increase tail and elevator effectiveness during transition. Acceleration to wing-supported flight is achieved by tilting the aircraft. Further details of the aircraft are presented in Reference 9.

2.5 Ryan XV-5A

The XV-5A (Fig. 5) is powered by two jet engines which drive two fans in the wing and one in the nose for VTOL lift. These engines provide direct thrust for cruise. VTOL roll control is provided by lift-fan thrust modulation, yaw control by differential wing-fan vectoring, and pitch control by nose-fan thrust modulation. Acceleration to wing-supported flight is provided by vectoring the main fan flow. Further details of the aircraft are presented in Reference 10.

3. TESTING

The wind-tunnel tests were performed in the Ames 40 ft by 80 ft Wind-Tunnel with similar test setups (e.g., see Figures 1-5) and procedures. However, the flight tests were carried out by various agencies which had various specific objectives. In none of

the wind-tunnel or flight tests was the prime objective to correlate wind-tunnel and flight-test results; thus the amount of data available for this correlation is limited.

3.1 Wind-Tunnel Testing

Aerodynamic and static-stability and control characteristics were all explored near balanced flight conditions. At discrete airspeeds, from 0 to wing-supported flight speed, data were obtained with lift equal to weight, drag equal to thrust, and moment equal to zero. Then angle of attack, angle of sideslip, power setting, and the various control settings were varied to determine the effect on each variable on aircraft characteristics. This type of wind-tunnel testing does not provide basic data but it is the fastest way of obtaining pertinent data about over-all aircraft characteristics.

3.2 Flight Testing

The flight tests were limited to steady-state conditions for approximately level flight and were further limited to avoid deep penetration into known problem areas. Flight work with the XV-3 and VZ-3 was done at Ames and an Ames representative was on hand during XV-5A flight tests, so the problems of coordinating and interpreting data were easily solved. The contractor supplied the applicable flight-test data that had been reduced for the XC-142 and the XV-4A, which resulted in a smaller amount of data being available for correlation because the major interest of the contractor was not a wind-tunnel flight-test correlation.

4. RESULTS AND DISCUSSION

4.1 Correlation of Wind-Tunnel and Flight-Test Results

Representative aerodynamic data from wind-tunnel and flight tests for the five aircraft are compared in the following section. Unless otherwise noted, none of the wind-tunnel data are corrected for wall effects. In most cases the comparison is made at steady-state, level flight conditions (lift equal to weight, thrust equal to drag).

4.1.1 XV-3

Power required for level flight, fuselage angle, and longitudinal control position for trim, both in flight and in the wind-tunnel, is shown as a function of airspeed in Figure 6. Power required as a function of airspeed shows excellent agreement, but angle of attack and longitudinal control data show scatter. Since accuracy in setting longitudinal control was $\pm 1^{o}$, and angle of attack is difficult to measure accurately in slow speed flight, the agreement between the two sets of data is good. Although the aircraft span was large with respect to the tunnel (Table 1), the disk loading was low (about 5 lb/ft^2), so that the wake deflection angle with respect to the vertical would be relatively large and thus the adverse effect of model size on wind-tunnel wall effects would be reduced.

4.1.2 VZ-3

Similar results (power required, angle of attack, and longitudinal control) are presented in Figure 7 for the deflected slipstream aircraft. Again power required for level flight showed excellent agreement between wind-tunnel and flight. A 23% increase

in horizontal tail area, added after the wind-tunnel tests, may have contributed to the fuselage angle of attack for trim being about 1^{o} greater in flight and the nose-down elevator for trim being about 2^{o} less in flight than in the wind-tunnel. This aircraft was small with respect to the wind-tunnel and the disk loading was moderate (20 lb/ft^{2}) so that wind-tunnel wall effects should be small.

The wind-tunnel data provided accurate assessments of the aircraft performance, stability, and control.

4.1.3 XC-142

Wing incidence angle for trimmed, level flight is presented in Figure 8 as a function of velocity. Wind-tunnel and flight-test results agree within 5^{o} for the wing-tilt angle required for 30 knots airspeed and within 2^{o} for 55 knots airspeed.

Descent rates obtained in flight and predicted from wind-tunnel data are presented in Figure 9 as a function of airspeed for several aircraft configurations. The flight-test data fall into two curves, one is the descent rate for buffet onset, and the other is the maximum descent rate as defined by small lateral-directional oscillations. The descent rates for buffet onset seem to agree with wind-tunnel data up to 45 knots airspeed at the higher wing-tilt angles. At higher airspeeds and lower wing-tilt angle the maximum descent rates that have been obtained in flight are much greater than those estimated from the wind-tunnel data. The descent rate estimated from the wind-tunnel data is based on when $C_{L_{max}}$ was first attained, or, in the cases noted, on the maximum angle of attack tested. It is unlikely that wind-tunnel wall effects are responsible for the discrepancy because of the better correlation of flight and wind-tunnel results at low speed. A more likely cause of difference is either low maximum lift of the model, or the aircraft flying beyond $C_{L_{max}}$ with no adverse effects. Model scale and low installed power combined to reduce Reynolds number to one-third of the full-scale value; this caused model Reynolds number to be in the region where maximum lift can be significantly affected, and can thus affect the correlation. Based on present knowledge, agreement is fair for trimmed level flight but poor for allowable descent angles.

4.1.4 XV-4A

Flight-test data were limited for this aircraft. Data are available only for transitions during which the aircraft was decelerating. Figure 10 shows the longitudinal acceleration, angle of attack, and elevator position as a function of airspeed during a transition. The angle of attack and elevator position for trim estimated from the wind-tunnel data to produce the equivalent deceleration in level flight are included on the figure. Angle of attack generally agreed to within 1^{o}, but elevator position varied by 4^{o} to 7^{o} (12% of maximum travel). The reason for the relatively poor correlation of elevator angle is not clear. The aircraft tested in the wind tunnel was not the same aircraft that supplied the flight-test data, so some of the difference could be based on differences in rigging or effectiveness of horizontal-tail boundary-layer control.

Both conventional wind-tunnel wall corrections and Heyson's corrections were applied to the XV-4A wind-tunnel data in an attempt to improve correlation with flight.

Figure 11 shows the XV-4A angle of attack for the same deceleration as in Figure 10, and as calculated from uncorrected wind-tunnel data (level flight was assumed), and from wind-tunnel data with conventional corrections and with Heyson's corrections. Conventional corrections increased the angle-of-attack discrepancy from 1^{o} to about 1.5^{o}. Heyson's corrections increased the discrepancy slightly.

4.1.5 XV-5A

Relative power, angle of attack, vector angle, and longitudinal stick position required for balanced flight are presented as a function of airspeed in Figure 12. The power required for level flight decreased as airspeed increased, indicating no "suckdown" effect and that lift increased with airspeed. Based on the results in Reference 11, a reduction of lift with airspeed would be expected. Although the flight-test data show considerable scatter due to small accelerations, the agreement between wind tunnel and flight is good. It should be noted that this aircraft was nearly twice the size of the XV-4A, and lifting element loading was about the same. The largest discrepancy between flight and wind-tunnel tests is in longitudinal stick position; the discrepancy is about 1^{o}, or 3% of the total stick travel.

Subsequent to these flights, the fairings at the wing-fan hub between the rotor blades were removed, which changed fan performance so that more power and additional vectoring were required for a given flight speed. Flight-test data with the revised fan configuration were obtained at constant airspeed and several angles of attack. The longitudinal stick position for trim as a function of angle of attack is presented in Figure 13 for three airspeeds. Good correlation is evident at 36 and 50 knots. Agreement is poor at 70 knots, indicating the static stability in the wind-tunnel was different from that measured in flight; the discrepancy would be further increased by wall corrections. At least a part of the failure to correlate at 70 knots is due to the sensitivity of pitching moment to vector angle at this airspeed. Because of the previously mentioned removal of the fairings, the vector angles in flight were from 1.5^{o} to 7^{o} greater than for the wind-tunnel results shown in Figure 13.

The XV-5A wind-tunnel tests showed an instability with angle of attack over part of the angle-of-attack range, the particular angle of attack for the occurrence being a function of the nose-fan thrust modulator position. Tests with and without nose-fan thrust modulation indicated that the cause of the instability was a reduction of tail effectiveness due to the flow from the nose-fan thrust modulator. In the flight tests, aircraft angle of attack was increased until the tail angle-of-attack indicator registered turbulent flow conditions; the test was then terminated. This flight-test angle-of-attack boundary and the wind-tunnel angle of attack for instability are presented in Figure 14. Considering the qualitative nature of the flight-test data, agreement is good, and flow conditions at the tail were accurately simulated in the wind-tunnel.

The effect of wind-tunnel wall corrections on the XV-5A wind-tunnel flight correlation is shown in Figure 15. In this case conventional wall corrections were nearly as large as Heyson's corrections. Corrections did not improve the correlation, although the effect on vector angle was small. The most significant effect was on power required; wall-effect corrections amounted to a 10% increase over that measured in flight.

The correlation between flight-test and wind-tunnel results for these five aircraft demonstrates the attainable accuracy in V/STOL wind-tunnel testing with aircraft to tunnel size ratios that approach values used for wind-tunnel tests of conventional aircraft. Correlation with uncorrected wind-tunnel data was good, with the possible exception of the XC-142 model, in spite of the difficulties associated with making accurate measurements at low speeds. It was also shown that, for the two cases examined, any wind-tunnel wall corrections degraded the correlation. For the majority of correlations of wind-tunnel with flight, the conditions considered were for lift equal to weight, and the thrust vectored to balance drag. Wall effects were reduced for these flight conditions, because the lifting element wake is deflected downstream more than it would be with drag unbalanced.

4.2 Wall-Effect Parameters

4.2.1 Present test results

The preceding section examined the accuracy of uncorrected wind-tunnel data for several aircraft of widely differing characteristics and sizes with respect to the wind-tunnel. Although the results are too incomplete to establish a definite criterion for maximum model to wind-tunnel size for V/STOL wind-tunnel testing, the model to wind-tunnel sizes have been shown to be acceptable by the results of the flight-test and wind-tunnel correlation. An attempt will now be made to correlate these results in terms of wind-tunnel wall-effect parameters. According to Reference 3, the pertinent model-tunnel sizing parameters are the lifting-element area to wind-tunnel cross-sectional area ratio, A_L/A_T , for VTOL concepts where the majority of the lift is supplied by the lifting elements, and the wing momentum area to tunnel cross-sectional area ratio, A_m/A_T , for concepts where the lift is distributed across the wing span. Study of Reference 1 also shows that lifting element wake deflection angle, which is a function of disk loading at a given airspeed (wake deflection angle = $f(V/V_j)$ = $f(V/\sqrt{T_F})$), is another important parameter. Disk loading is an important parameter for all V/STOL aircraft and provides a common basis for comparison. Accordingly, area ratio is plotted versus disk loading in Figure 16 for the five test aircraft.* Both suggested area ratios are included for all five aircraft. Since the XV-3 and XV-5A are two extremes of disk loading and have only small wall effects, lines have been drawn through these data points. The area underneath the lines should indicate acceptable model sizing. The point for the XC-142, which appears above the line, has unresolved questions concerning the correlation, and it may be that this model is too large for the wind tunnel. The wind-tunnel and flight correlation was acceptable for the VZ-3 and XV-4A, and the data points for these aircraft fall below the line. It should be emphasized that the use of straight lines on Figure 16 is somewhat arbitrary.

The single lines shown in Figure 16 connect points for two aircraft which were tested in the wind-tunnel at different minimum speeds; the aircraft with the lower disk loadings showed good agreement to speeds as low as 20 knots, whereas for the higher disk loadings it was difficult to get reliable data below 30 knots because blockage and recirculation made it difficult to set steady-state test conditions. Additional

---

* Other common parameters, such as disk loading to dynamic pressure ratio, velocity ratio V/V_j, or wake deflection angle were considered for the presentation. However, they were not used because of the assumptions that are required for the calculation of these parameters. Furthermore, these parameters obscure the wide range of disk loading represented by the composite data from the several aircraft.

data may show that separate 20 and 30 knot boundaries should be drawn on the figure, rather than the single boundary for the two constant airspeeds. The acceptable maximum model size for a given wind-tunnel should decrease with decreasing minimum test airspeed. The boundaries drawn on Figure 16 probably approximate a practical test boundary because the need for wind-tunnel data between 0 and 30 knots depends on disk loading; the low disk loading aircraft will fly a larger percentage of the time at low speeds and will be more sensitive to gusts or small maneuver velocities than the higher disk loading aircraft at the lower forward speeds.

4.2.2 Comparison of boundaries with other results

Small-scale results, from testing the same model in different wind-tunnel test sections[2, 3], were analyzed in an attempt to further document the boundaries on Figure 16. For all models, the model tunnel size ratio in the smallest test section approached conventional values and test conditions were near the boundary lines of Figure 16. The model data were allowed a 5% lift error at low speed (when evaluated with thrust equal to drag) in order to simulate accuracy comparable to the probable accuracy of the data in the preceding wind-tunnel flight-test correlation. The uncorrected tilt-wing data from the 7 ft by 10 ft wind-tunnel, presented in Reference 3, were well within the 5% margin for balanced flight at low speed. Uncorrected lift data from a helicopter rotor tested in large and small test sections[2] also agreed within 5% for balanced flight at low speed. Reference 3 did not present balanced flight data for the lift-fan configurations, so it was necessary to use data that corresponded to large aircraft decelerations. Unlike the other two models, the two lift-fan configurations in the smallest test sections showed a sizable lift error, so that it was necessary to plot both the fan-in-fuselage and fan-in-wing lift errors in the various wind-tunnel test sections as a function of model to wind-tunnel size ratio in order to determine the area ratio for a 5% lift discrepancy. This method has a further uncertainty because the models were tested in wind-tunnels with different width-to-height ratios. The appropriate model to wind-tunnel size ratios of these four models is compared with the wind-tunnel flight-test correlation boundaries on Figure 17. The two model tests at the lower disk loadings indicate no conflict between the full-scale results (the lines on Figure 17) and the model tests; however, for the higher disk-loading models a decided discrepancy is evident. At least a part of the discrepancy can be explained by failure to balance model drag, so that the wake deflection angle is less for these models than for the similar aircraft. If Heyson's corrections are taken as an indication of the importance of wake deflection angle, balancing the drag reduces the calculated wall corrections to as little as 50% of the value with the drag unbalanced. A change in this direction would tend to reduce the discrepancy between the high disk loading small-scale results and the wind-tunnel flight-test correlation. Another possible cause of the discrepancy is the span being large relative to wind-tunnel width; this subject is discussed in the next section.

4.2.3 Test section geometry

The wind-tunnel flight-test correlation is based on tests in a wind-tunnel with a 2 to 1 width-height ratio, which is a larger ratio than any of the test sections used in the small-scale tests. This test section geometric parameter has a direct bearing on span to tunnel width ratios, which are an important parameter in conventional wind-tunnel wall corrections and may also be important for V/STOL model testing. This ratio is presented in Figure 18 as a function of disk loading for the aircraft in the full-scale correlation and for the models in References 2 and 3 installed in their smallest

test section. The aircraft and models that indicated insignificant corrections have conventional span to wind-tunnel width ratios at low disk loadings and relatively small span to width ratios at high disk loadings. The two small-scale lift-fan models that indicated large wind-tunnel wall corrections had larger span to width ratios than the comparable aircraft. These results suggest that another boundary line in addition to those in Figure 16, indicating acceptable span to tunnel width ratio, may be appropriate to specify the effects of test-section geometry when sizing a V/STOL model. The effect of wind-tunnel cross-section geometry on wall effects should be studied experimentally since it may significantly influence V/STOL wind-tunnel data.

In summary, although some of the results presented in Reference 2 disagree with the results presented here for model-tunnel sizing parameters, adequate reasons for the disagreement exist. For the conditions considered in the present report (i.e., realistic flight conditions and allowable errors no larger than data measurement errors), the model to wind-tunnel size ratios, as indicated by the boundary lines on Figures 16 and 18, which are larger than previously considered usable, should give acceptable wind-tunnel results for V/STOL model testing. All three boundaries should be regarded as constraints for a given model to insure good test results.

5. CONCLUDING REMARKS

In order to obtain satisfactory data from V/STOL wind-tunnel testing in the low-speed flight range, it is necessary to successfully resolve the conflict in model sizing caused by the need to minimize both wall effects and scale effects. In Reference 3, scale effects were shown to be larger than the effect of Heyson's corrections in some cases, but in other cases (the XV-4A, 0.18 scale, $A_L/A_T = 0.01$) were shown to be negligible. Thus careful planning of test programs is required in order to minimize the possibility of obtaining erroneous or misleading test data.

The three tentative boundaries obtained from the results of the correlation of wind-tunnel and flight-test aerodynamic data for five different V/STOL concepts indicate that the model-tunnel sizing ratios can approach the values used for conventional aircraft, depending on the test velocity desired and the disk loading of the propulsion system. For testing requiring data acquisition at lower velocities or at higher disk loadings than considered herein, smaller values of model to wind-tunnel size ratios will be necessary, whereas for STOL testing larger values of the sizing ratios should be acceptable. The models should be as large as possible because Reynolds number effects can be critical for inlets, high lift devices and the characteristics of propellers, fans and compressors. The disk loading and flow distribution of the lifting elements should approximate full-scale characteristics to minimize secondary effects of Reynolds number. Tests at conditions closely related to realistic flight values of acceleration and deceleration minimize the magnitude of wind-tunnel wall effects and enable larger scale models to be utilized in wind-tunnels. Instrumentation sufficient to determine the performance of the various model components, including the lifting elements, is useful in detecting substandard performance of the components due to low Reynolds number or failure to realistically simulate the aircraft or lifting element disk loading.

REFERENCES

1. Heyson, Harry H. — *Linearized Theory of Wind-Tunnel Jet-Boundary Corrections and Ground Effect for VTOL-STOL Aircraft.* NASA TR R-124, 1962.

2. Lee, Jerry Louis — *An Experimental Investigation of the Use of Test Section Inserts as a Device to Verify Theoretical Wall Corrections for a Lifting Rotor Centered in a Closed Rectangular Test Section.* Thesis for Masters Degree, University of Washington, 1964.

3. Davenport, Edwin E. Kuhn, Richard E. — *Wind-Tunnel Wall Effects and Scale Effects on a VTOL Configuration With a Fan Mounted in the Fuselage.* NASA TN D-2560, 1965.

4. Grunwald, Kalman J. — *Experimental Study of Wind-Tunnel Wall Effects and Wall Corrections for a General-Research V/STOL Tilt-Wing Model With Flap.* NASA TN D-2887, 1965.

5. Powered-Lift Aerodynamics Section Staff — *Wall Effects and Scale Effects in V/STOL Model Testing.* Paper at AIAA-Navy Aerodynamic Testing Conference, 1964.

6. Koenig, David G. et alii — *Full-Scale Wind-Tuunel Investigation of the Longitudinal Characteristics of a Tilting-Rotor Convertiplane.* NASA TN D-35, 1959.

7. James, Harry A. et alii — *Wind-Tunnel and Piloted Flight Simulator Investigation of a Deflected-Slipstream VTOL Airplane, the Ryan VZ-3RY.* NASA TN D-89, 1959.

8. Deckert, Wallace H. et alii — *Large-Scale Wind-Tunnel Tests of Descent Performance of an Airplane Model With a Tilt Wing and Differential Propeller Thrust.* NASA TN D-1857, 1964.

9. – — *Lockheed Hummingbird Preliminary Aircraft Specification.* Lockheed Document ER-5180M, May 1961.

10. – — *Lift-Fan Flight Research Aircraft Program, Airplane Detail Specification.* Specification 118A, General Electric Company, Flight Propulsion Laboratory Department., Cincinnatti, Ohio, April 1963.

11. Spreemann, Kenneth P. — *Induced Interference Effects on Jet and Buried-Fan VTOL Configurations in Transition.* NASA Conference on V/STOL Aircraft, 1960.

TABLE I.

Aircraft Geometry with Respect to the Wind-Tunnel

Aircraft	*Type*	$\frac{A_L}{A_T}$	$\frac{A_m}{A_T}$	$\frac{b}{b_T}$	$\frac{T}{A_L}$
XV-3	Tilt rotor	0.291	0.758	0.656	5.6
VZ-3	Vectored slipstream	0.046	0.151	0.292	19.9
XC-142	Tilt wing	0.095	0.451	0.506	50*
XV-4A	Jet ejector	0.0077	0.186	0.325	300
XV-5A	Lift fan	0.0149	0.244	0.372	275

* Full-scale disk loading only; model disk loading was 15 lb/ft^2.

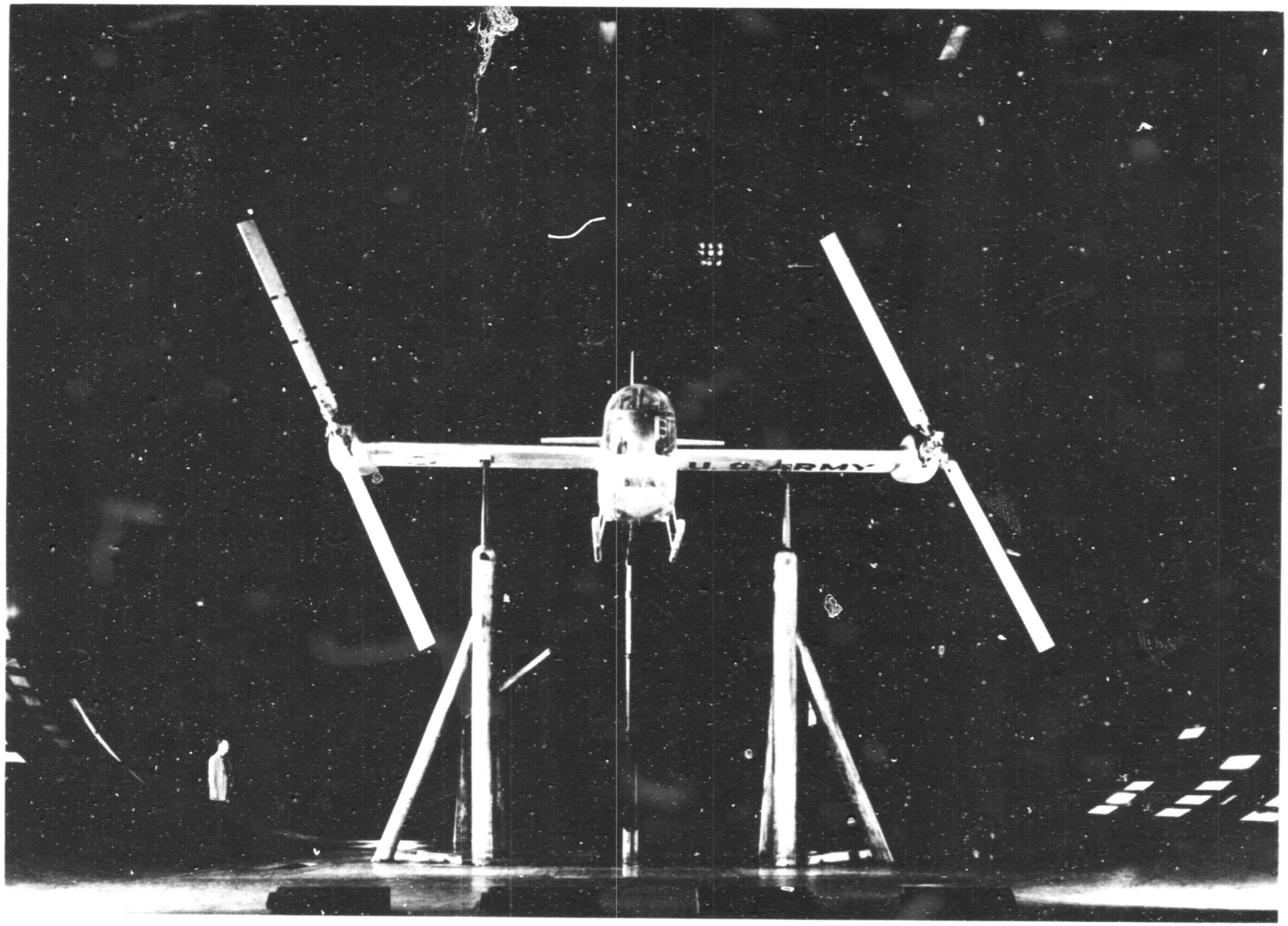

Fig. 1 The Bell XV-3 mounted in the Ames 40 ft by 80 ft wind-tunnel

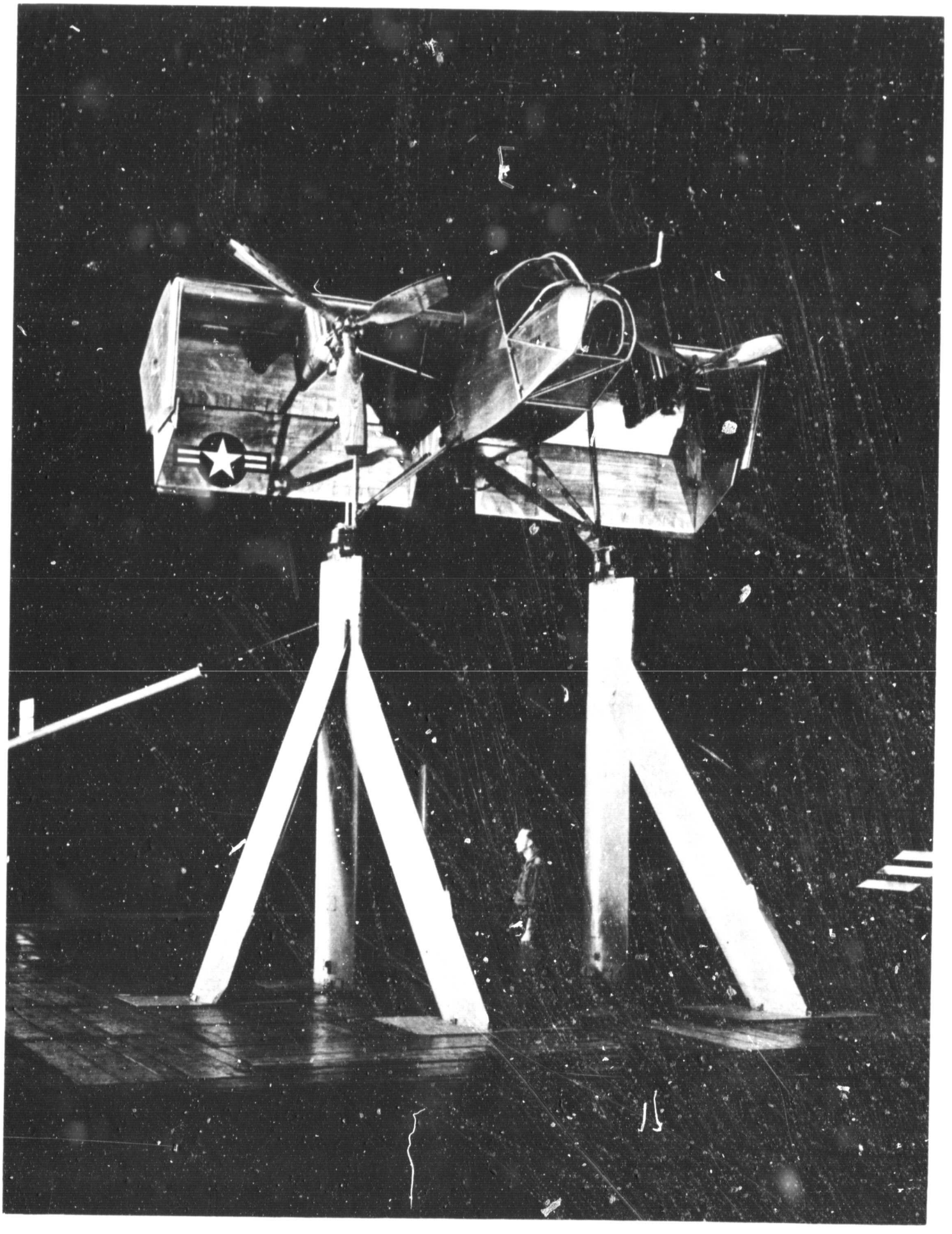

Fig. 2 The Ryan VZ-3 mounted in the Ames 40 ft by 80 ft wind-tunnel

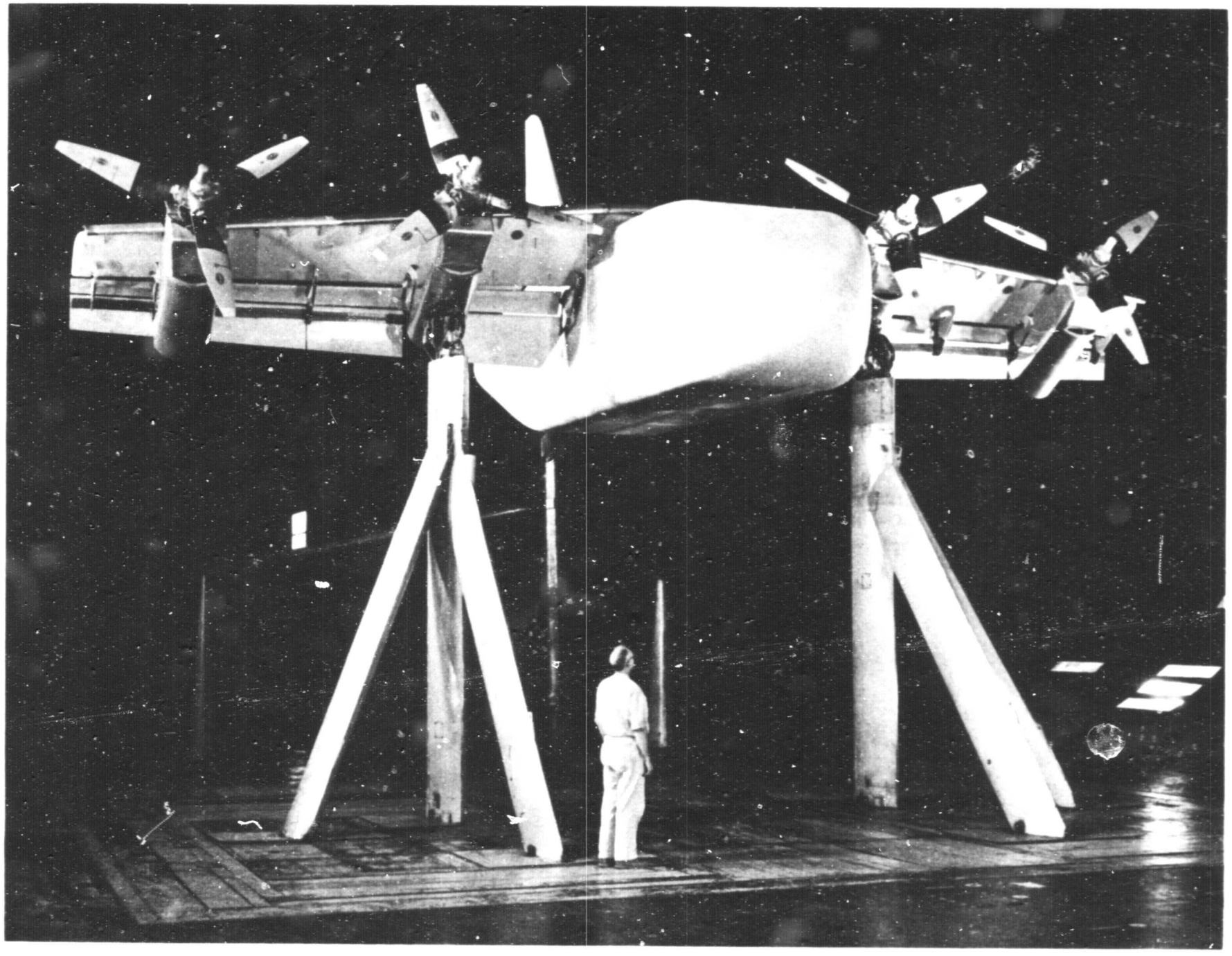

Fig. 3 The LTV XC-142 model mounted in the Ames 40 ft by 80 ft wind-tunnel

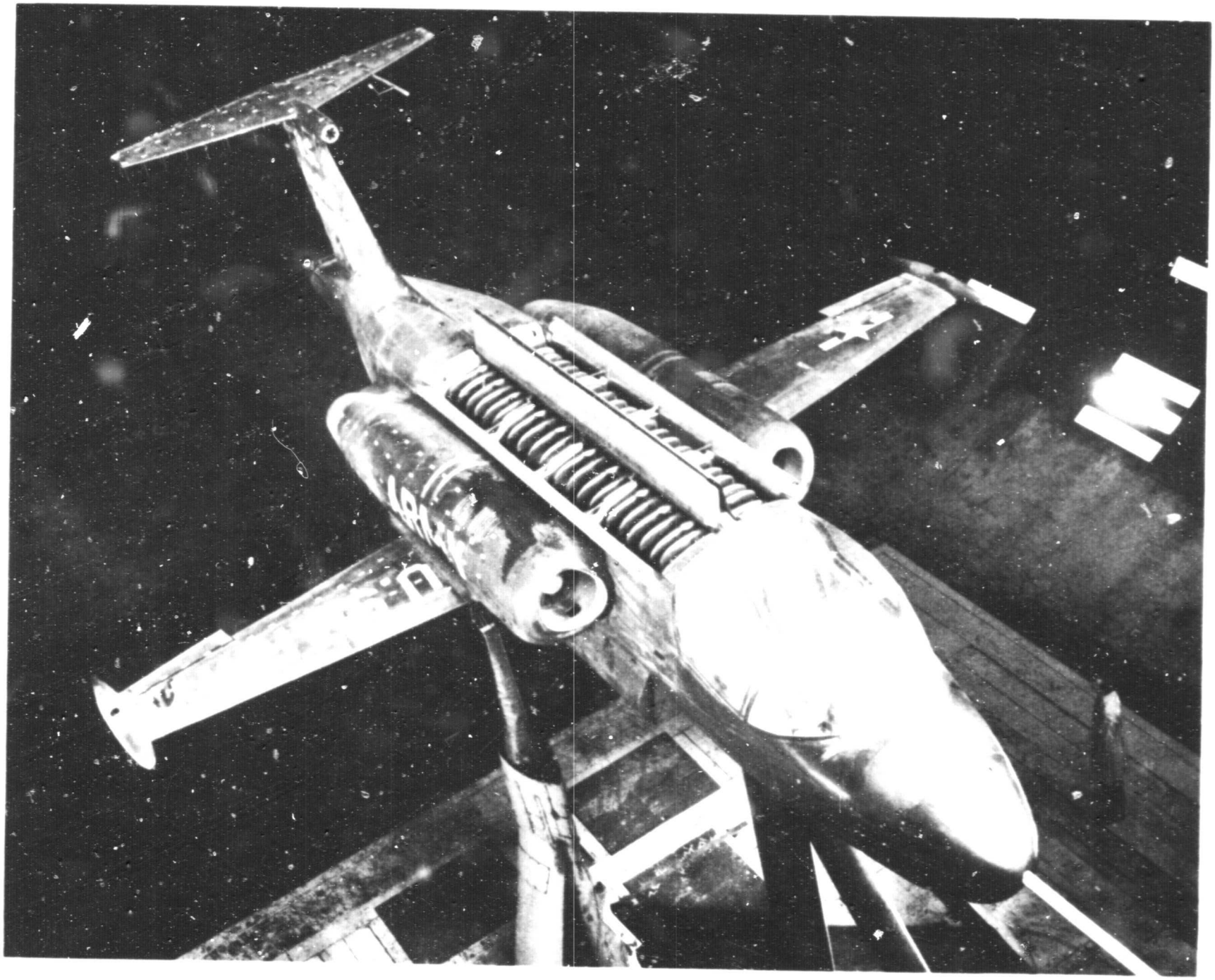

Fig.4 The Lockheed XV-4A mounted in the Ames 40 ft by 80 ft wind-tunnel

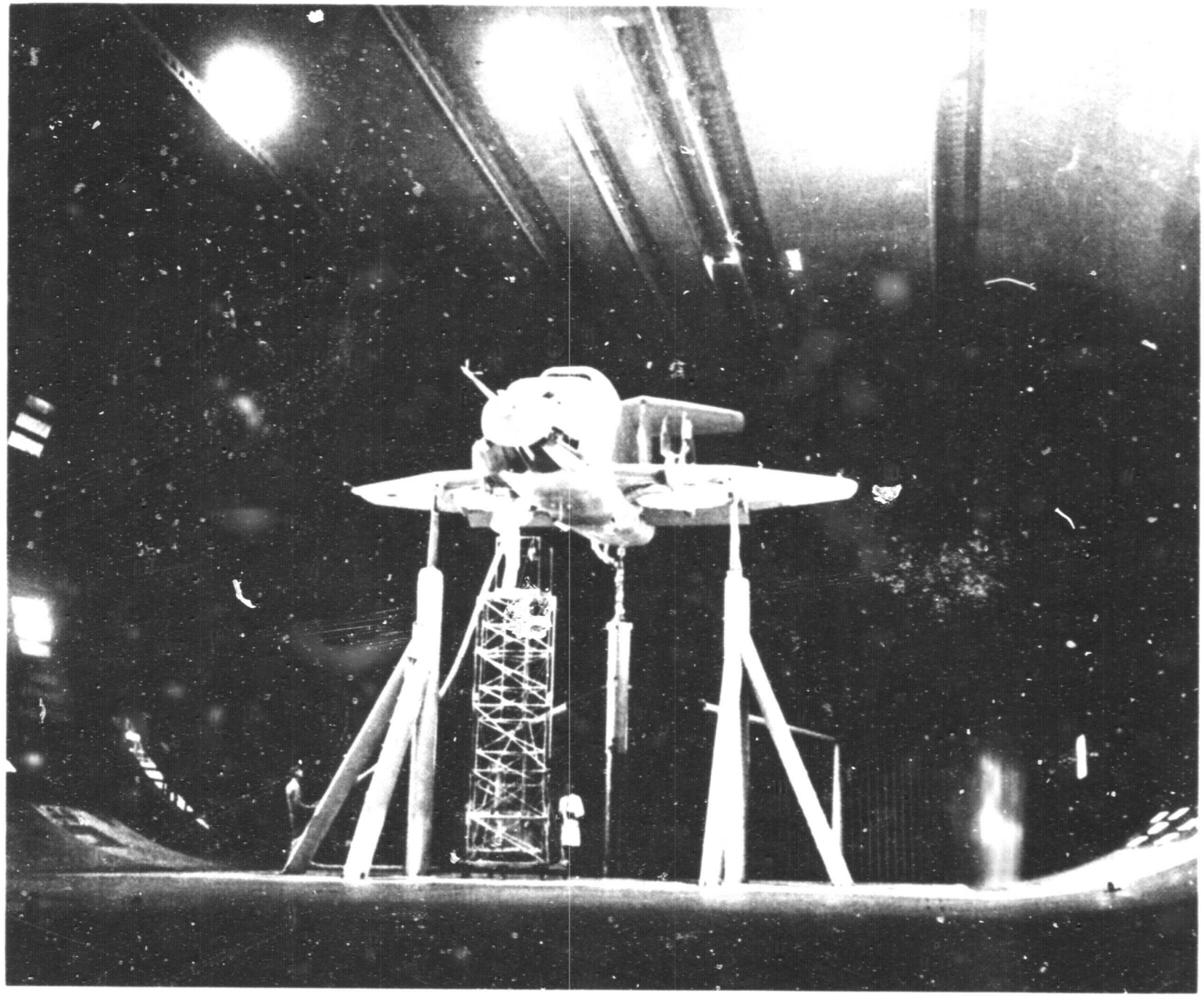

Fig.5 The Ryan XV-5A mounted in the Ames 40 ft by 80 ft wind-tunnel

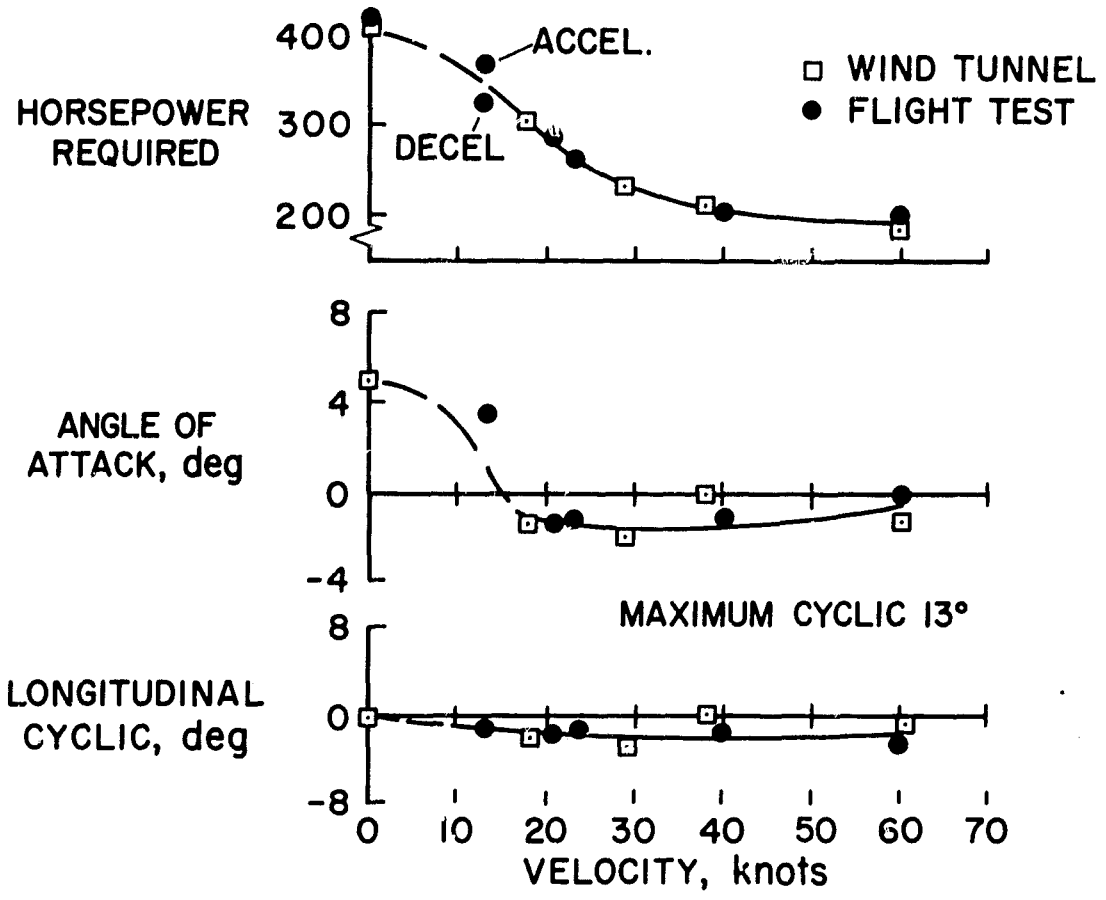

Fig.6 Balanced, level flight characteristics of the XV-3 convertiplane

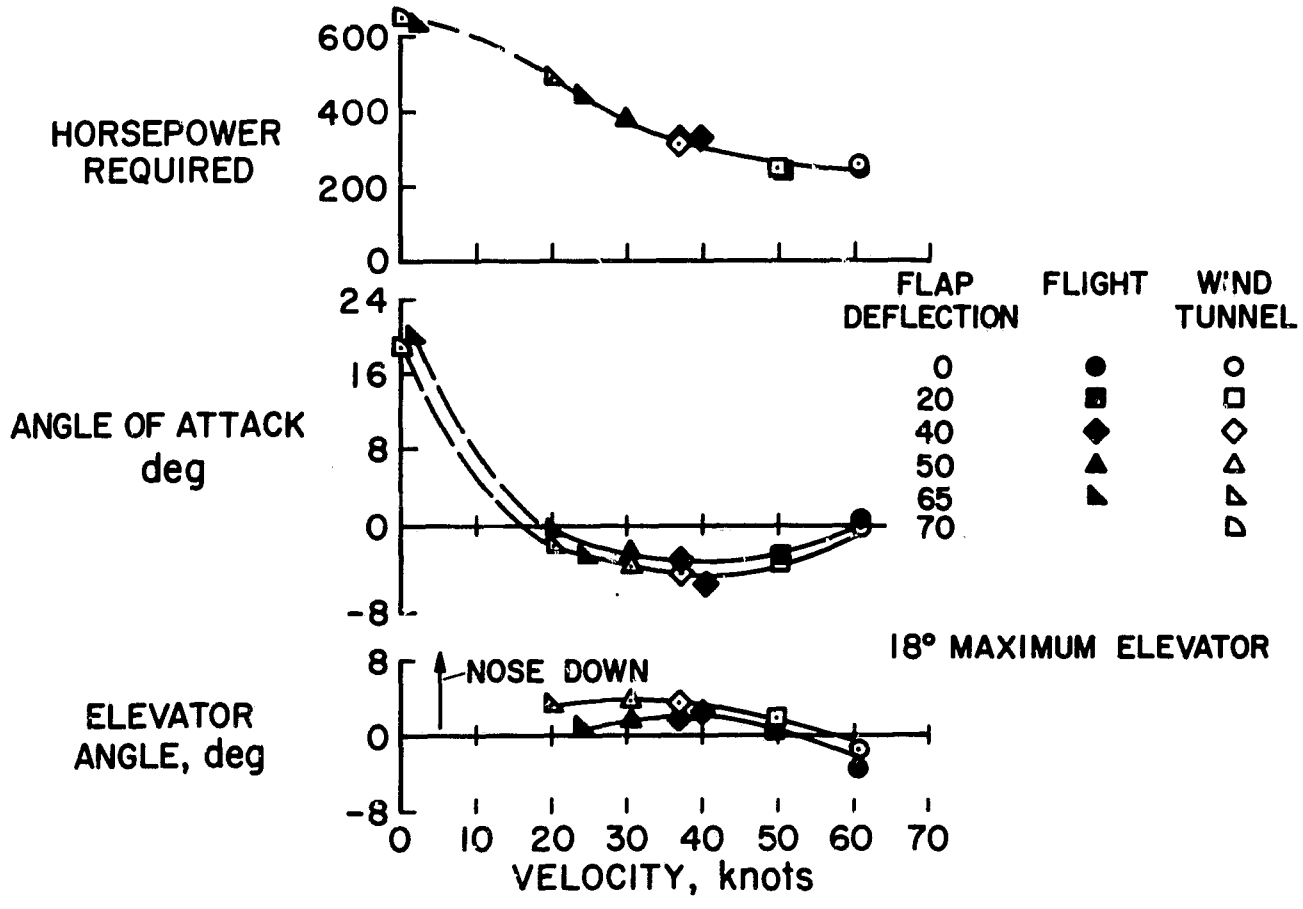

Fig.7 Balanced, level flight characteristics of the VZ-3 aircraft

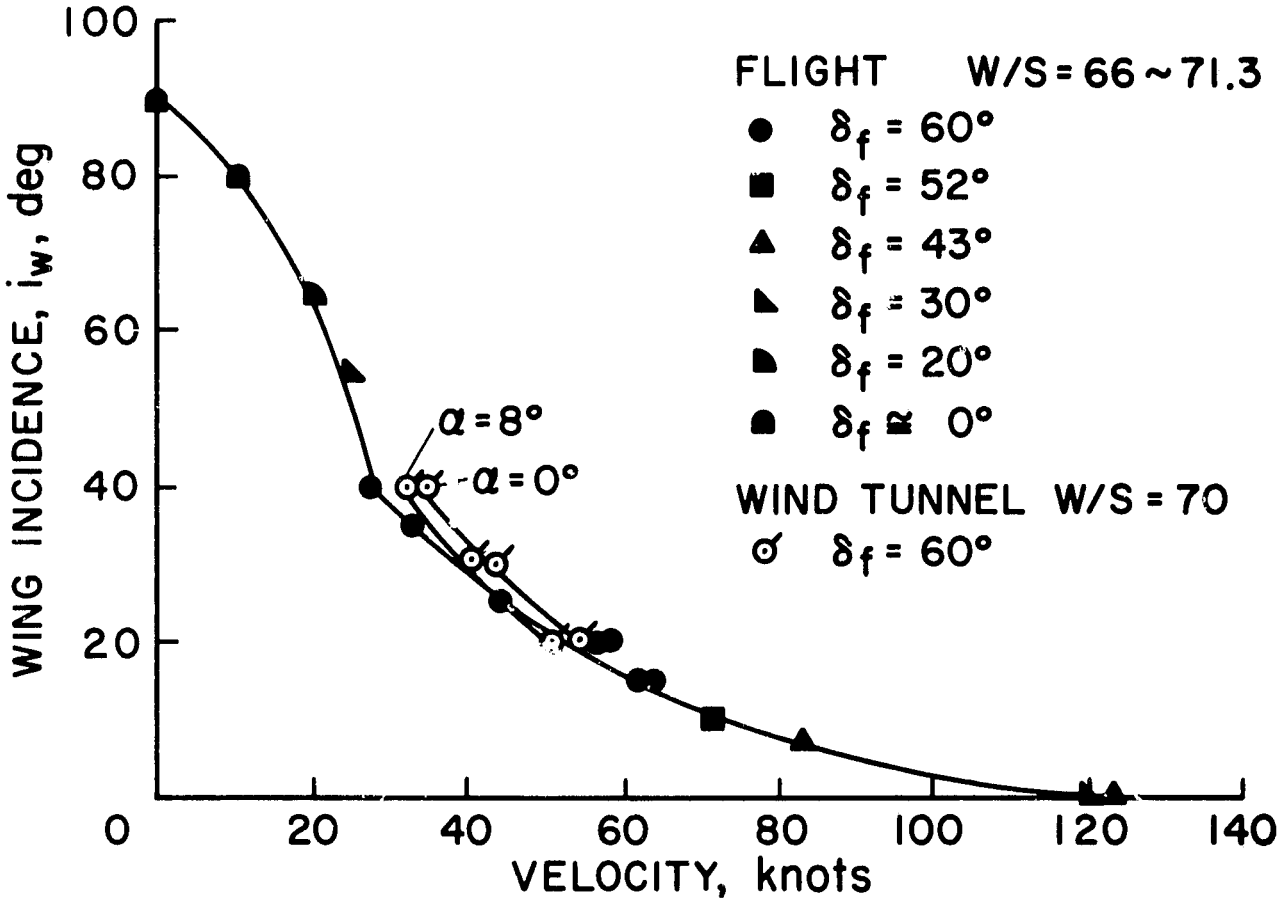

Fig.8 Wing-tilt angle for balanced, level flight of the XC-142

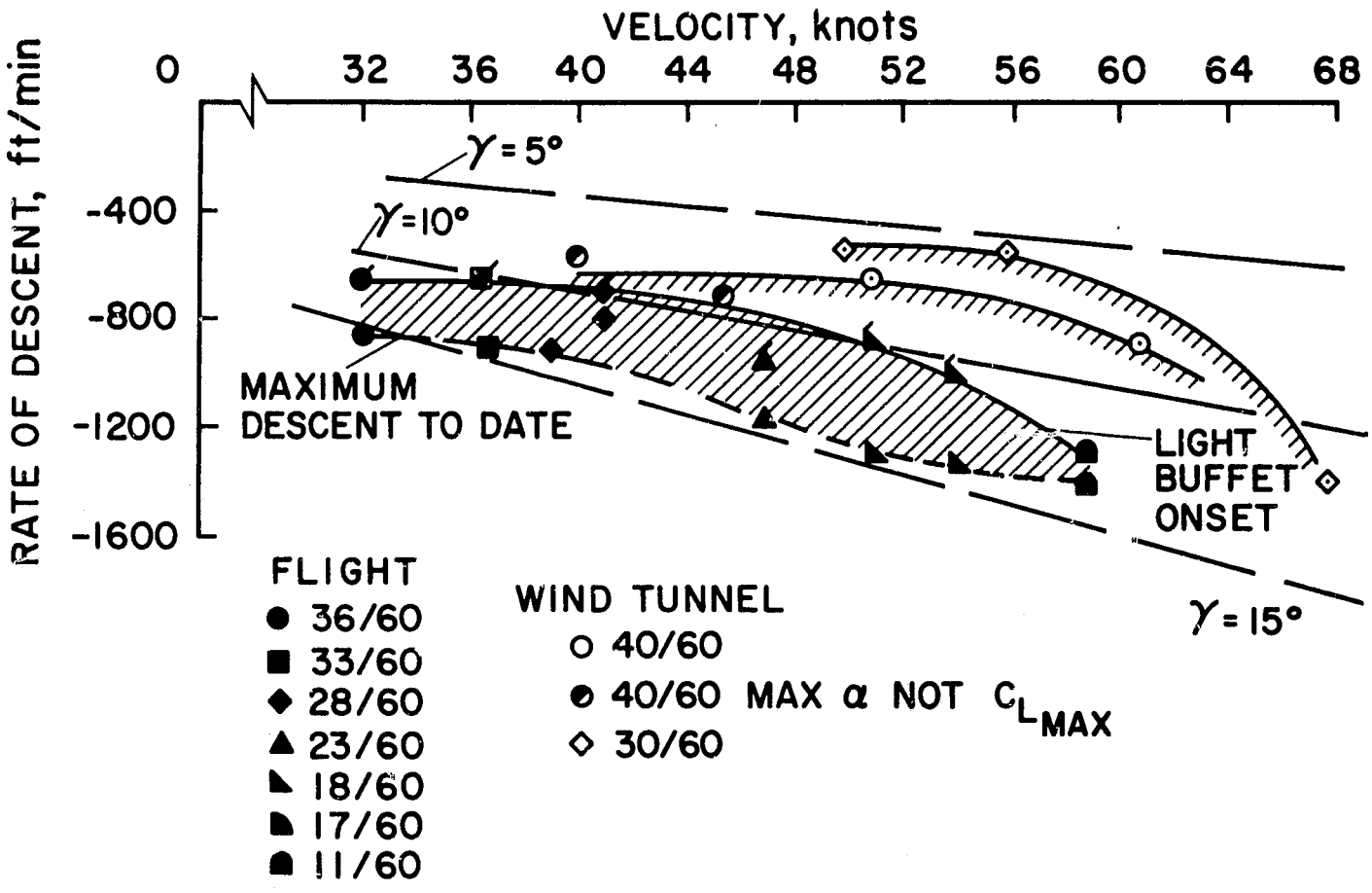

Fig.9 Descent boundaries for the XC-142

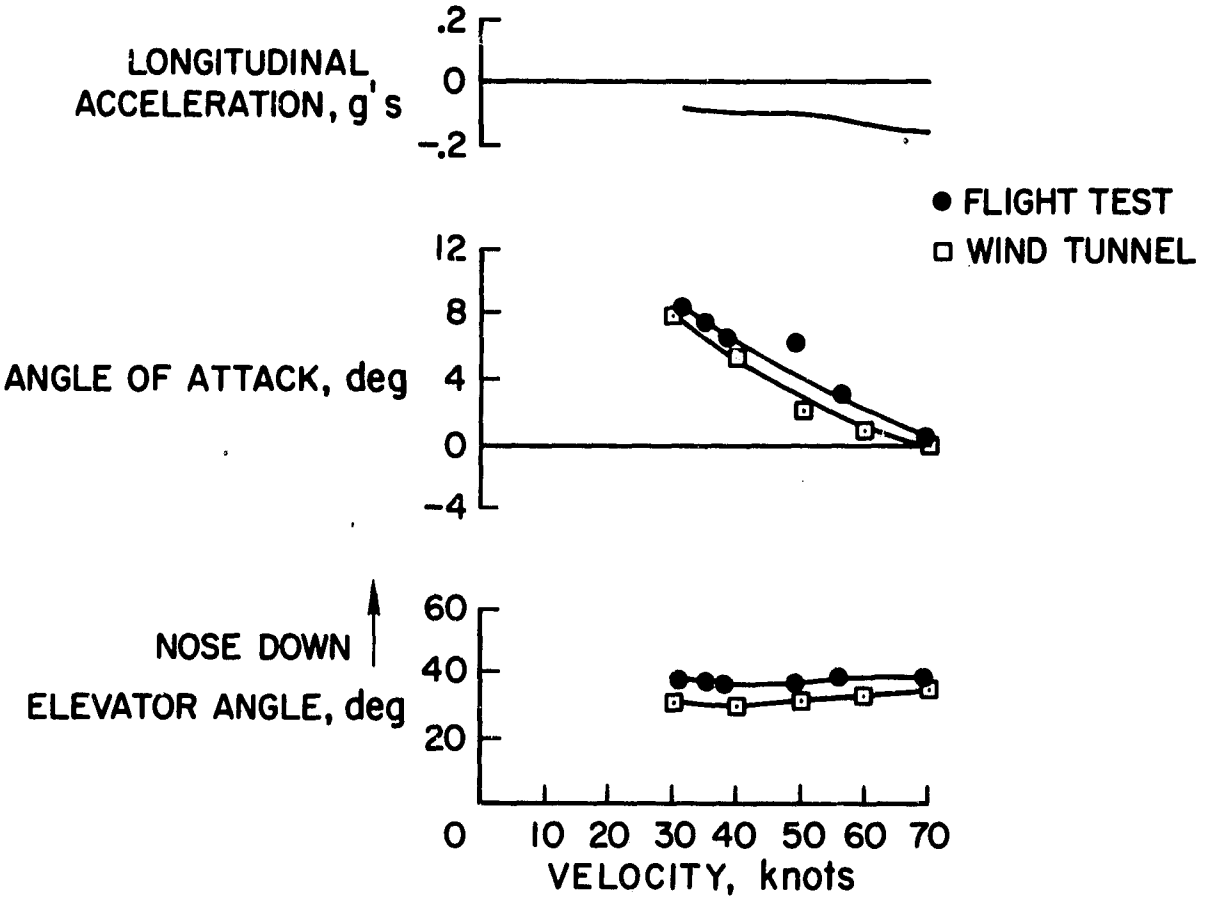

Fig. 10 Characteristics of the XV-4A

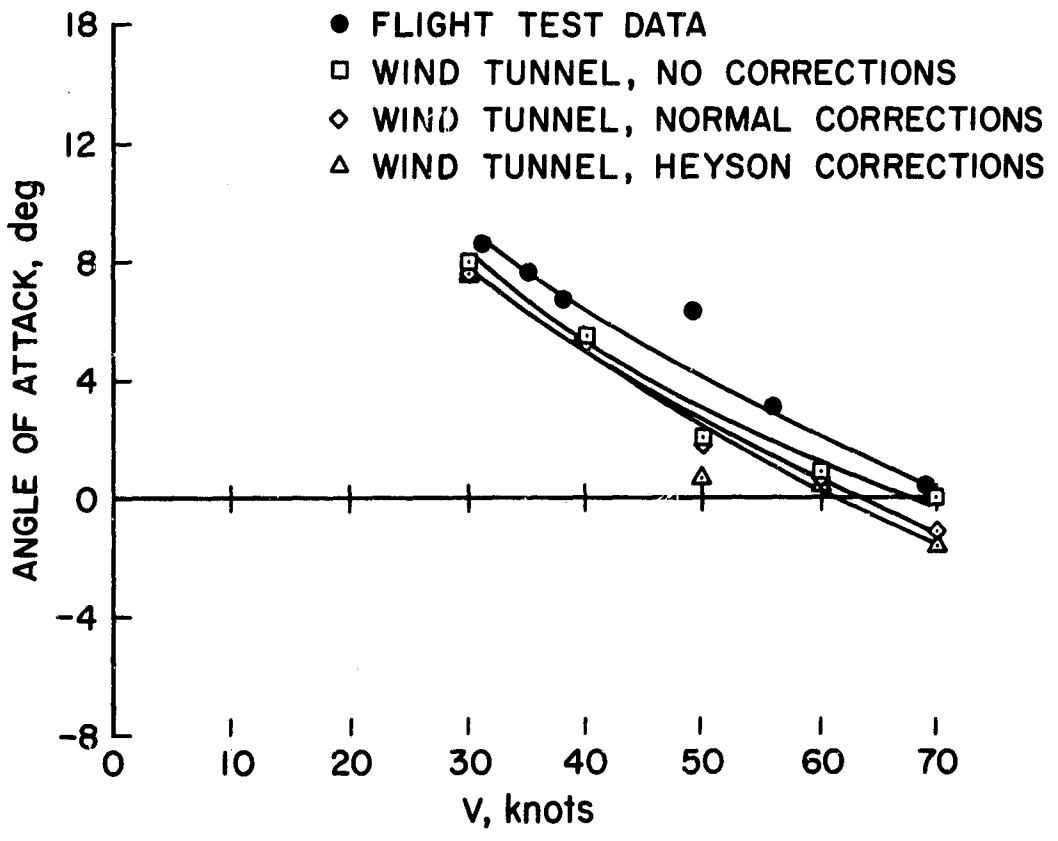

Fig. 11 The effect of wind-tunnel wall corrections on the correlation between wind-tunnel and flight-test results for the XV-4A

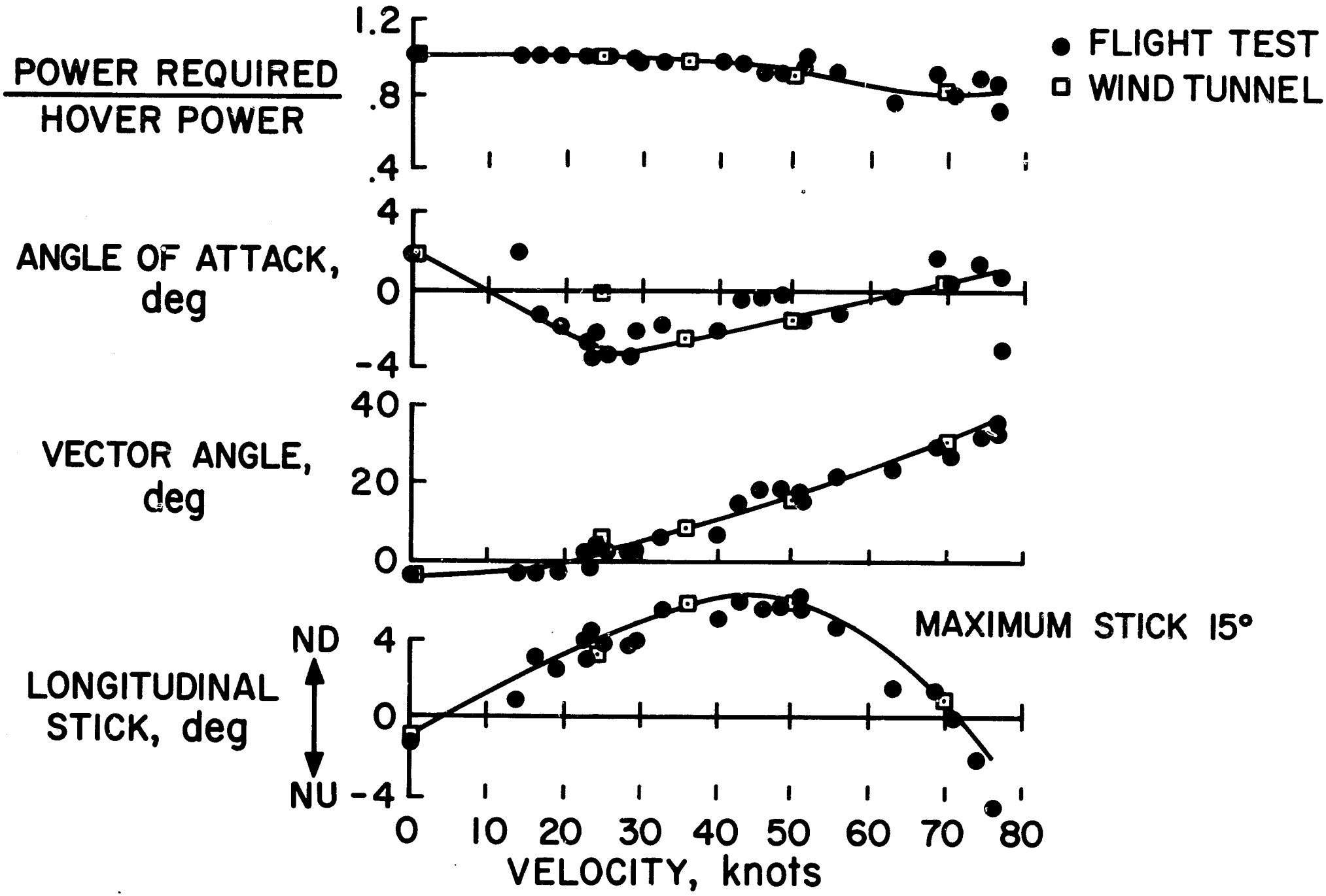

Fig.12 Balanced, level flight characteristics of the XV-5A

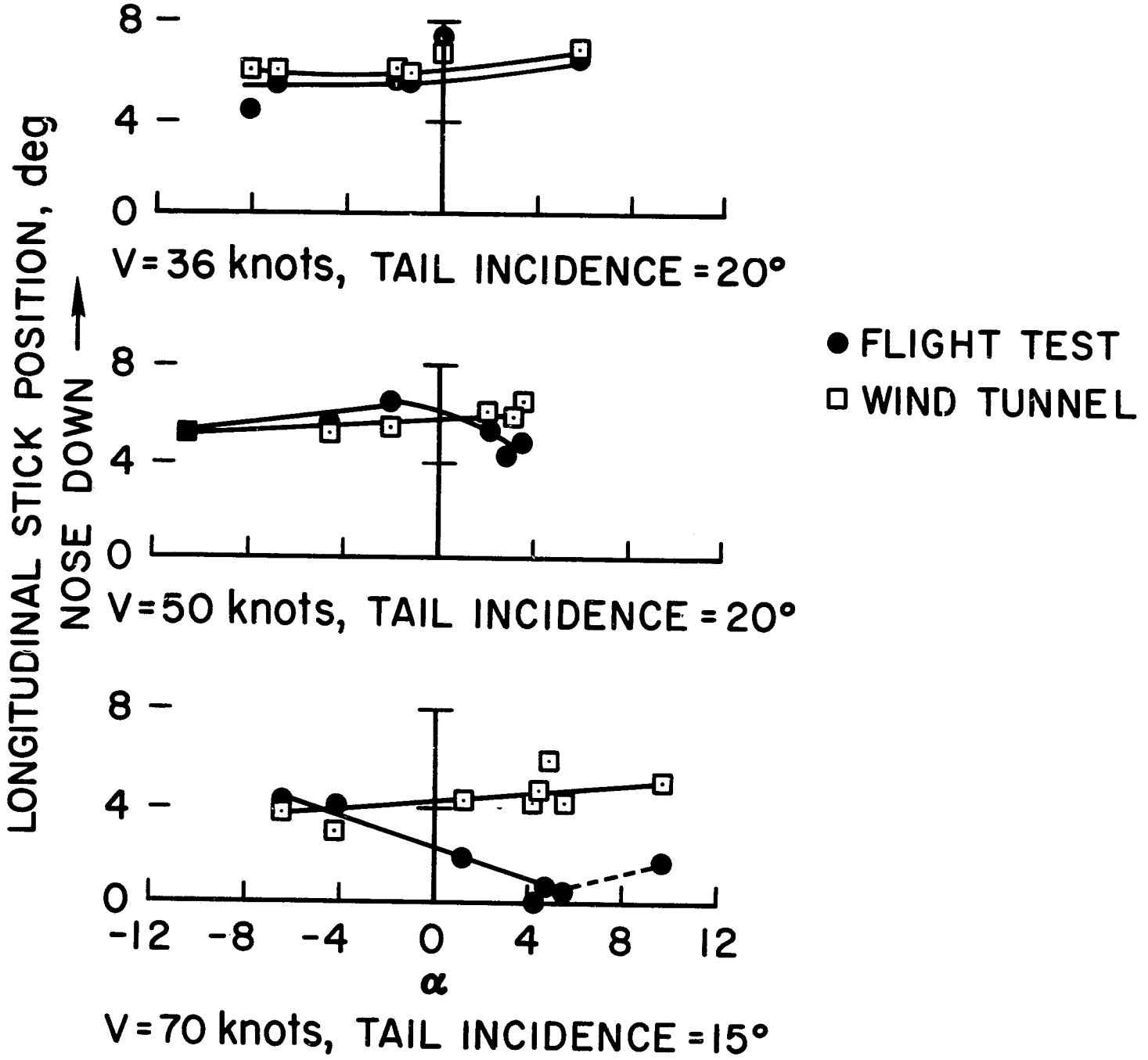

Fig.13 The variation with angle of attack of longitudinal stick position for trim for the XV - 5A aircraft in flight and in the wind-tunnel

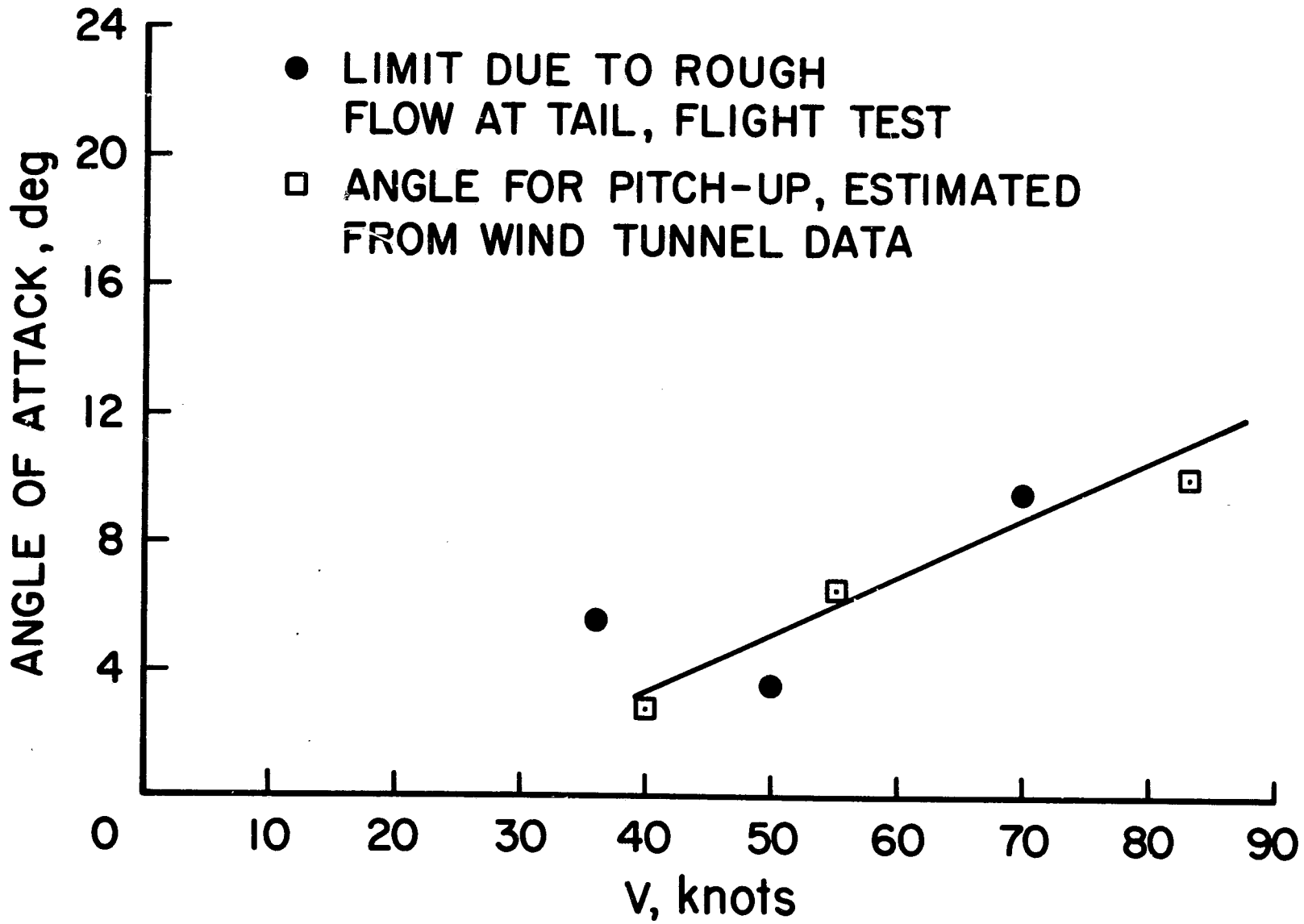

Fig.14 Angle of attack for instability for the XV-5A in flight and in the wind-tunnel

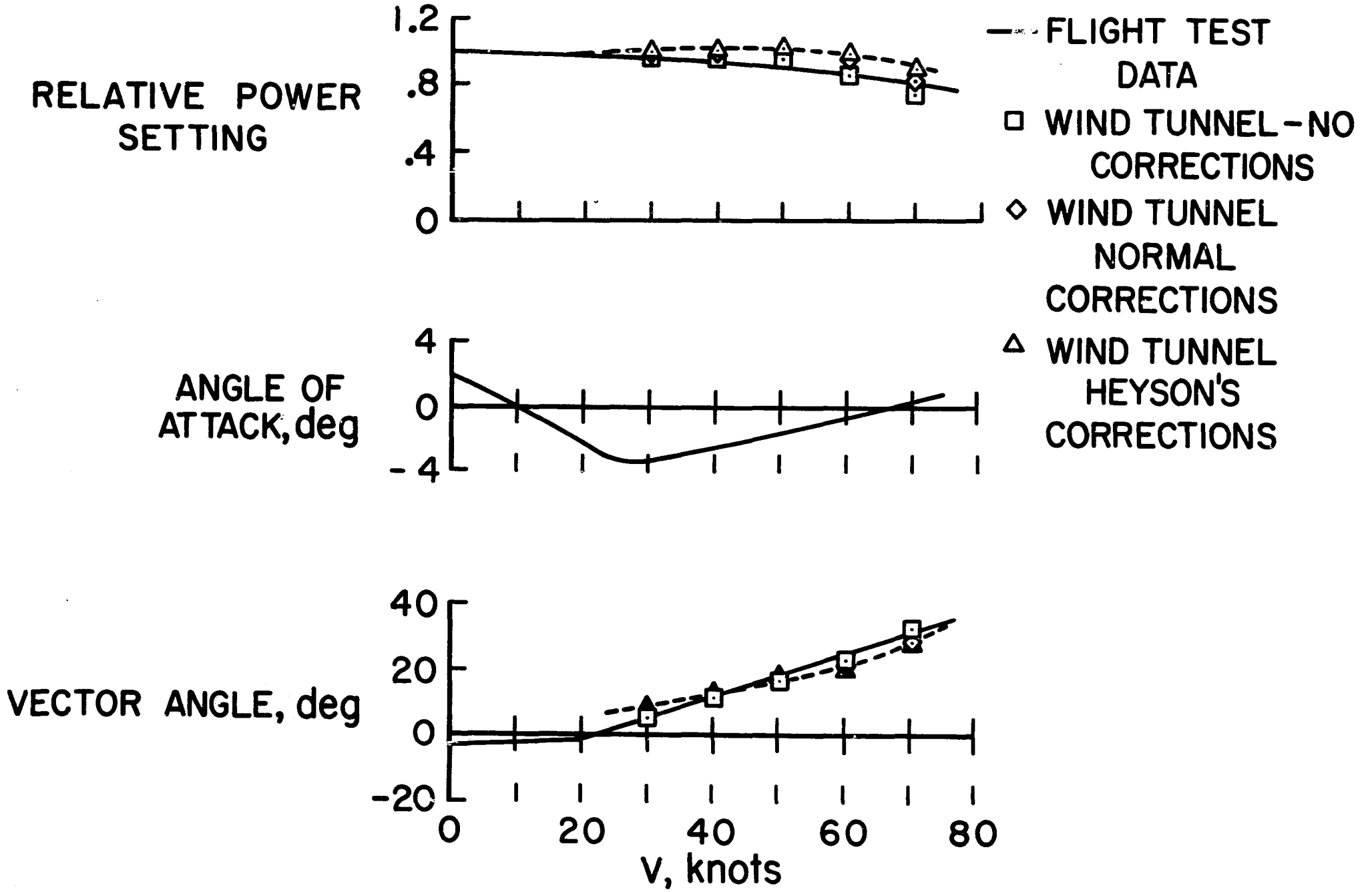

Fig. 15 Effect of wind-tunnel wall corrections on correlation between wind-tunnel and flight test for the XV-5A aircraft

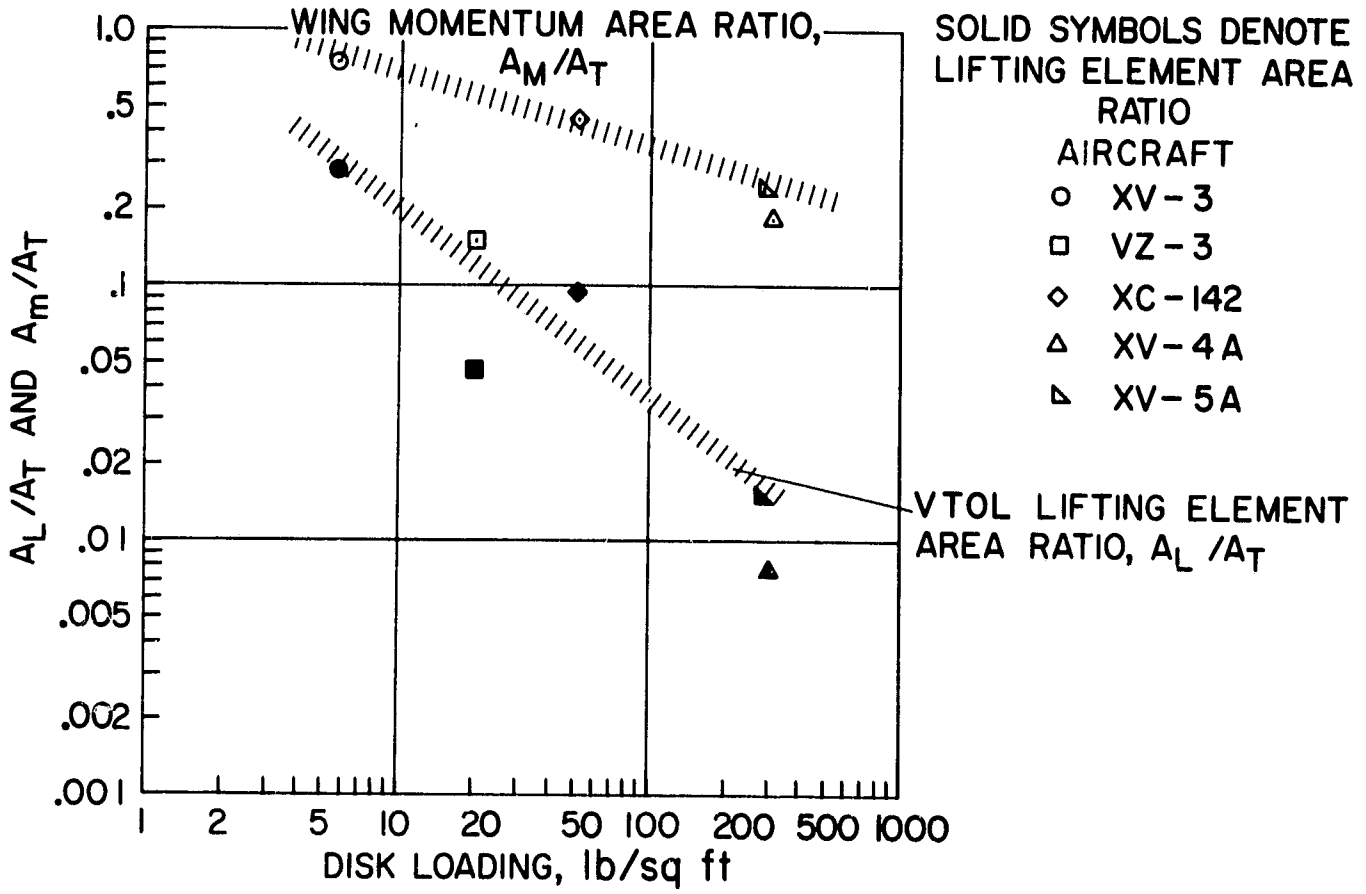

Fig. 16 The variation of aircraft to wind-tunnel size ratios with disk loading

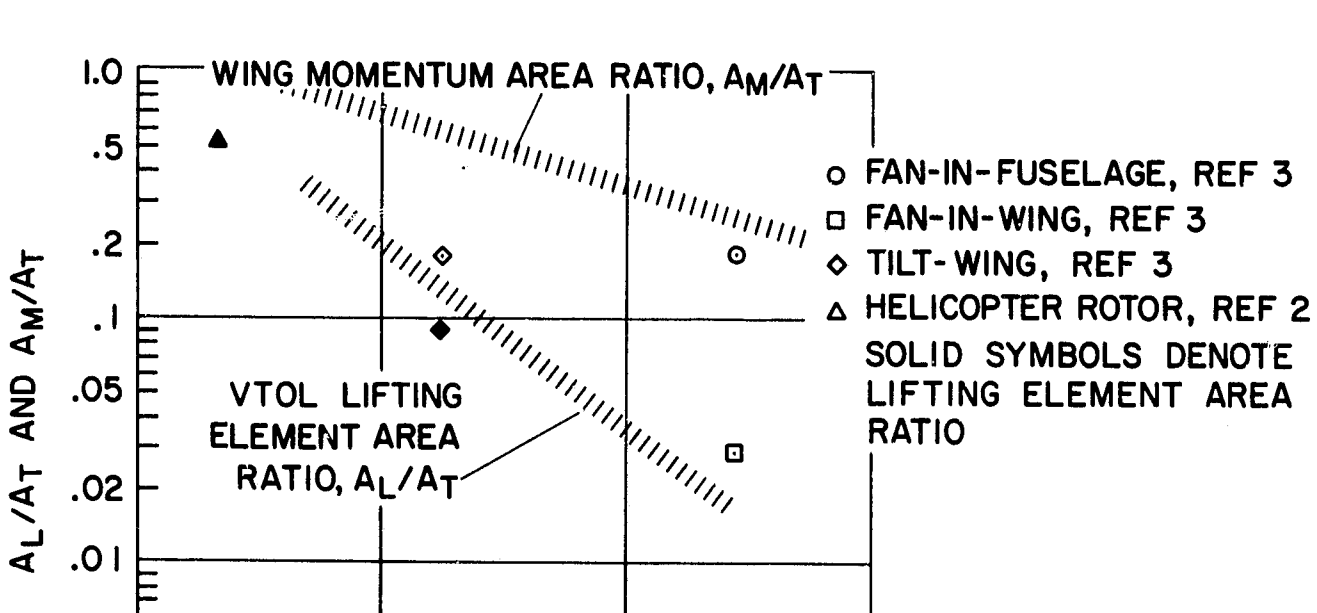

Fig. 17 The variation of small-scale model to wind-tunnel size ratios with disk loading

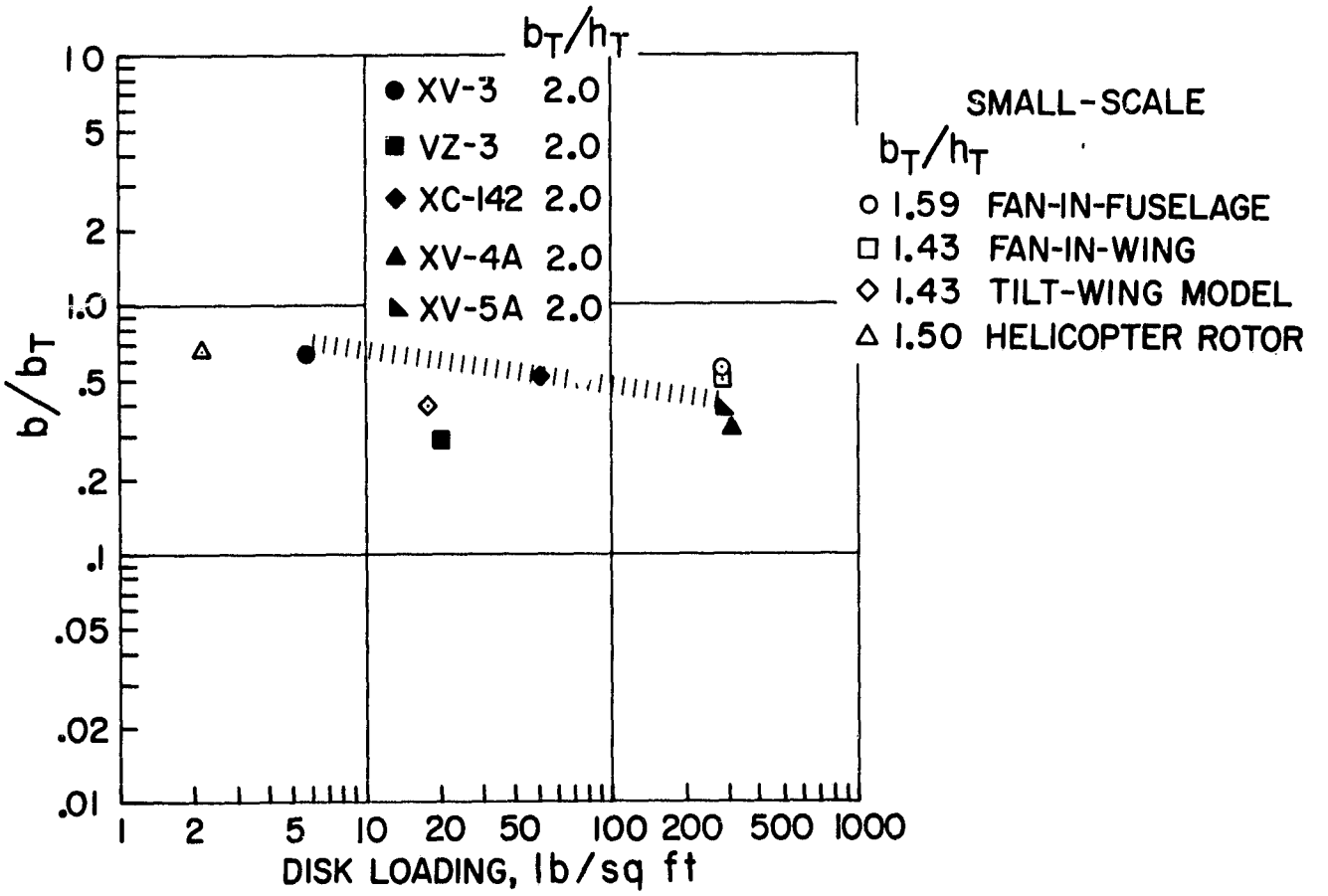

Fig. 18 Aircraft and model span (wind-tunnel width) ratios

DISTRIBUTION

Copies of AGARD publications may be obtained in the various countries at the addresses given below.

On peut se procurer des exemplaires des publications de l'AGARD aux adresses suivantes.

BELGIUM BELGIQUE	Centre National d'Etudes et de Recherches Aéronautiques 11, rue d'Egmont, Bruxelles
CANADA	Director of Scientific Information Service Defence Research Board Department of National Defence 'A' Building, Ottawa, Ontario
DENMARK DANEMARK	Danish Defence Research Board Østerbrogades Kaserne, Copenhagen, Ø
FRANCE	O.N.E.R.A. (Direction) 25, Av. de la Division Leclerc Châtillon-sous-Bagneux (Seine)
GERMANY ALLEMAGNE	Zentralistelle für Luftfahrtdokumentation und Information 8 Munchen 27 Maria-Theresia-Str. 21 Attn: Dr. H.J. Rautenberg
GREECE GRECE	Greek National Defence General Staff B.JSG, Athens
ICELAND ISLANDE	Director of Aviation c/o Flugrad, Reykjavik
ITALY ITALIE	Ufficio del Delegato Nazionale all'AGARD Ministero Difesa – Aeronautica Roma
LUXEMBURG LUXEMBOURG	Obtainable through Belgium
NETHERLANDS PAYS BAS	Netherlands Delegation to AGARD Kluyverweg 1, Delft

NORWAY NORVEGE	Norwegian Defence Research Establishment Kjeller per Lillestrom Attn: Mr. O. Blichner
PORTUGAL	Delegado Nacional do 'AGARD' Direcção do Serviço de Material da Forca Aerea Rua da Escola Politecnica, 42 Lisboa
TURKEY TURQUIE	Ministry of National Defence Ankara Attn: AGARD National Delegate
UNITED KINGDOM ROYAUME UNI	Ministry of Aviation T.I.L., Room 135 Leysdown Road, Mottingham, London S.E.9.
UNITED STATES ETATS UNIS	National Aeronautics and Space Administration (NASA) Washington, D.C. 20546

Printed by Technical Editing and Reproduction Ltd
Harford House, 7-9 Charlotte St. London. W. 1.